Damascus University Journal of Earthquake and Disaster Research
Vo 1 number (1) -2024: 79-90

مجلة جامعة دمشق لبحوث الزلازل والكوارث
المجلد1 العدد(1) – 2024: 79-90

Dynamic Behavior of Buried Structures Under the Effect of Surface Explosions Using Nonlinear Numerical Modelling

ALI Adnan Khadra*[1] Hala Hasan[2] Turki Tabak[3] Ibrahim Hammoud[4]

*[1]. Higher Institute of Earthquake Studies and Research- Damascus University – Syria
ali.khadra@damascusuniversity.edu.sy
[2]. prof. at Higher Institute of Earthquake Studies and Research- Damascus University – Syria
hala.hasan@damascusuniversity.edu.sy
[3]. Scientific Studies and Research Center of Aleppo.
turkitabak@Damascusuniversity.edu.sy

[4]. prof. at Faculty of Civil Engineering- Damascus University – Syria
IbrahimHammoud@Damascusuniversity.edu.sy

Received: 31/5/2023

Accepted: 14/6/2023

Abstract:

Massive earthquakes and terrorist attacks cause destructive dynamic loads on the surface and buried structures and have been receiving increased attention due to recent damages witnessed over the world. This paper attempts to evaluate the effects of a possible surface blast on a buried reinforced concrete structure by analyzing its dynamic response with one complete model in which the explosion, shock wave propagation through the soil medium, the interaction of the soil with the buried structure, and the structure response itself using the ABAQUS/Explicit finite element package. To simulate soil behavior, the elastoplastic Drucker-Prager Cap model is utilized. The blasting process is simulated using the Jones-Wilkens-Lee equation of state, and the Concrete Damaged Plasticity model is used to simulate the behavior of concrete with reinforcement which is a flexible plastic material. To simulate the interface between the soil and the structure, the general concept of Mohr-Coulomb friction is used; This allows for sliding, separating, and rebounding of the structure's surface to the surrounding soil. Many parameters influence the optimization of structure design, for example; lining reinforcement ratio and construction depth. As the reinforcement ratio or structure depth increase, the peak of lining displacements decreases remarkably but with residual final ones which indicate a possible damage occurrence. Damage evaluation informs that increasing the reinforcement ratio might achieve a limited loss of elements strength, but with an appropriate depth, the structure might be completely safe.

Keywords: ground surface explosion, numerical simulation, dynamic behavior, soil-structure interaction, buried structure.

السّلوك الدّيناميكي للمنشآت المطمورة تحت تأثير الانفجارات السّطحيّة باستخدام النّمذجة العدديّة اللّا خطّيّة

علي عدنان خضره*[1] هالة حسن[2] تركي طبقْ[3] ابراهيم حمّود[4]

*[1].طالب ماجستير، مهندس في قسم الهندسة الإنشائيّة الزّلزاليّة، المعهد العالي للبحوث والدّراسات الزّلزاليّة، جامعة دمشق، سورية.

ali.khadra@damascusuniversity.edu.sy

2. أستاذ، دكتورة، مهندسة في قسم الهندسة الإنشائيّة الزّلزاليّة، المعهد العالي للبحوث والدّراسات الزّلزاليّة، جامعة دمشق، سورية.

hala.hasan@damascusuniversity.edu.sy

3. دكتور، مهندس، باحث في مركز الدّراسات والبحوث العلميّة، حلب، سورية.

turkitabak@Damascusuniversity.edu.sy

4. أستاذ، دكتور، مهندس في قسم الهندسة الجيوتكنيكيّة، كلّيّة الهندسة المدنيّة، جامعة دمشق، سورية.

IbrahimHammoud@Damascusuniversity.edu.sy

الملّخص:

تتسبّب الزّلازل الهائلة والهجمات الإرهابيّة بأحمال ديناميكيّة مدمّرة على المنشآت السّطحيّة والمطمورة، وقد حظيت دراستها باهتمام متزايد في الآونة الأخيرة بسبب الأضرار الّتي وقعت في أنحاء العالم جميعها.

تقدّم هذه المقالة تقييماً لآثار انفجار سطحي محتمل على منشأ مطمور، وذلك بتحليل استجابته الدّيناميكيّة وفق نموذج عددي واحد متكامل يتضمّن: الانفجار، انتشار موجة الصّدمة عبر وسط التّربة، تفاعل التّربة مع المنشأ المطمور، واستجابة المنشأ نفسه باستخدام حزمة العناصر المحدودة ABAQUS/Explicit. لمحاكاة سلوك التّربة استُخدِم نموذج (Elastoplastic Drucker–Prager Cap)، وتمّت محاكاة عمليّة التّفجير باستخدام معادلة الحالة (Jones–Wilkens–Lee)، بينما استُخدِم نموذج (Concrete Damaged Plasticity) لمحاكاة سلوك الخرسانة المسلّحة. لتمثيل سطح الاتّصال بين التّربة والمنشأ المطمور استُخدِم المبدأ العام (Mohr–Coulomb friction): الّذي يسمح بالانزلاق، الانفصال، والارتداد لسطح المنشأ إلى التّربة المحيطة. تؤثّر العديد من العوامل في التّصميم الأمثل للمنشأ، على سبيل المثال؛ نسبة تسليح البطانة الخرسانيّة وعمق التّشييد. بازدياد نسبة التّسليح أو عمق المنشأ، تنخفض ذروة انتقالات البطانة انخفاضاً ملحوظاً مع وجود انتقالات متبقّية نهائيّة ما يوحي بحدوث ضرر محتمل.

يشير تقييم الضّرر أنّ زيادة نسبة تسليح البطانة قد تؤدّي إلى خسارة محدودة في مقاومات العناصر الإنشائيّة، ولكن مع اختيار عمق التّشييد المناسب، يمكن الوصول إلى منشأ آمن كلّيّاً.

الكلمات المفتاحية: انفجار سطحي أرضي، نمذجة عدديّة، سلوك ديناميكي، تفاعل تربة_منشأ، منشأ مطمور.

تاريخ الايداع: 2023/5/31

تاريخ القبول: 2023/6/14

Introduction:

Verifying the dynamic response and safe design of structures subjected to destructive dynamic loads, such as sturdy seismicity movements and explosions, is always a critical matter to the diversity of engineering disciplines, specific structural and geotechnical engineering. The buried facilities are vital in all countries and used for various civil purposes, such as metro tunnels that bind cities for transportation and trade exchange, or may be used for strategic purposes, for example, nuclear power plants, and military fortifications. Three methods are distinguished for analyzing the dynamic behaviors of facilities under explosion loads: theoretical solutions, experimental study, and numerical methods. Generally, all previous methods should involve: (1) the explosion phenomena, (2) the propagation of blast loads through the transporter medium, (3) the dynamic response of the facility, and (4) the material damage of its elements (Yang et al. 2010). Theoretical solutions are usually difficult to achieve, especially for buried facilities, even with simplistic hypotheses. Experimental ones might be available covertly and exclusively to some government agencies and are uncommon in the open literature. Therefore, numerical methods that simulate the whole system (explosive _ soil _ structure) are necessary to enhance the predictions. Recently, the rapid evolution of numerical methods has provided strong support for studying buried facilities under dynamic loads, among which is the finite element method (FEM). In this paper, due to the recommendations of previous studies (Nagy et al. 2010, Nagy. 2015, Yang et al. 2010), a numerical investigation is performed to study the effects of structure depth and lining's reinforcement ratio on the dynamic response of the structure due to surface explosion. To this aim, a parametric study has been accomplished using the ABAQUS/EXPLICIT program with a complete coupled model that employs nonlinear material models to represent the realistic behavior of the problem. A numerical example is used to simulate the behavior of the whole suggested system (Nagy et al. 2010, Nagy. 2015).

1- Numerical Model:

2.1- Background and Finite Element Model:

The numerical model presents a two-dimensional symmetrical case study presented by (Nagy et al. 2010). Three materials are distinguished representing the model, namely the explosive charge, the structure lining, and the surrounding soil. The TNT explosive charge with a mass of (100 kg) is above the roof slab center of the structure. The structure is modeled as a cylindrical reinforced concrete lining with a constant thickness (t = 0.5 m), internal height (h = 3 m), and radius (r = 4 m). The depth of the structure (d_i) has two different values as a study parameter as shown in Fig.1(a) (Nagy et al. 2010), and the reinforcement ratio of the concrete lining varies between the minimum and maximum ratios adopted by (Code, S. E. B. 2004) as another study parameter in the investigation. The Arbitrary Lagrange Euler Coupling formulation (ALE) is utilized where expected high deformation is to eliminate mesh distortion (i.e. the explosive and near extended soil region) (Hu et al. 1998, Nagy et al. 2010), while the conventional Finite Element Method (FEM) is used for the whole system. The 4-node bilinear axisymmetric quadrilateral, reduced integration, elements (CAX4R) are used to represent the entire explosive - soil - structure, while the infinite elements (CINAX4) are used to provide quiet boundaries at the right-hand side and bottom boundaries of the mesh as shown in Fig.1(b) (Nagy et al. 2010).

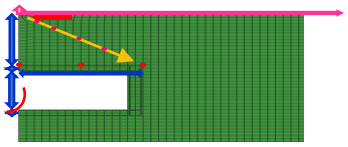

(a): Case Study

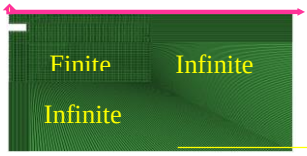

(b): Finite Element Mesh

Fig(1)The Case Study Diagram and Finite Element Mesh (Nagy et al. 2010)

2.2- Material Constitutive Models and Parameters

2.2.1- Explosive Model:

The TNT explosive charge is modeled by the Jones-Wilkins-Lee (JWL) high explosive equation of state, which expresses the pressure generated by the release of chemical energy in an explosive (Systèmes. 2014). The JWL equation of state can be written in terms of the internal energy per unit mass, E_{m0} as:

$$p = A\left(1 - \frac{\omega\rho}{R_1\rho_0}\right)exp\left(-R_1\frac{\rho_0}{\rho}\right) + B\left(1 - \frac{\omega\rho}{R_2\rho_0}\right)exp\left(-R_2\frac{\rho_0}{\rho}\right) + \frac{\omega\rho^2}{\rho_0}E_{m0}$$

Where A, B, R_1, R_2, and ω are the equation coefficients, with ρ_0 being the density of the explosive and $\boldsymbol{\rho}$ being the density of the products of detonation. The initial relative density $\frac{\rho_0}{\rho}$ is assumed to be unity, which means the initial specific energy E_{m0} with nonzero values should be specified. The parameters presented by (Nagy et al. 2010, Nagy. 2015), are adopted in this investigation, as shown in Table.1.

Table (1) Parameters of the TNT Explosive Charge (Nagy et al. 2010, Nagy. 2015)

Parameter	Value
Wave speed of detonation, C_d	6930 (m/s)
A	373800 (MPa)
B	3747 (MPa)
R_1	4.15
R_2	0.9
ω	0.35
Explosive density, ρ_0	1630 (kg/m^3)
Initial specific energy E_{m0}	3.63 (J/kg)

2.2.2- Soil Model:

The soil is modeled by the elastoplastic Drucker-Prager Cap model. The yield surface has two principal segments: a pressure-dependent Drucker-Prager shear failure segment F_S which is a perfectly plastic yield surface (i.e. no hardening), and a compression cap segment F_C which provides an inelastic hardening mechanism. A transition surface F_t provides a smooth surface between the shear failure surface and cap segment, as shown in Fig (2) (Systèmes. 2014). The parameters adopted for this model as presented in (Nagy. 2015), and shown in Table.2.

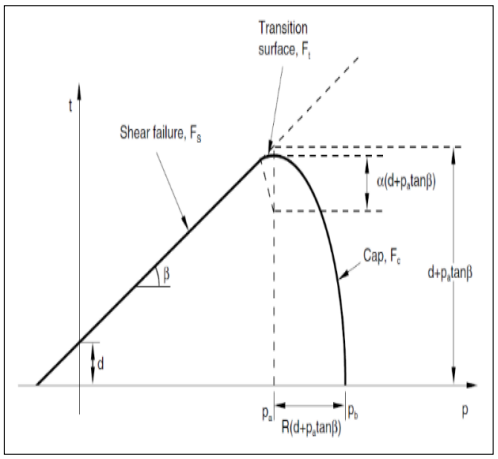

Fig (2) Drucker _Prager Cap Model (Systèmes. 2014)

Table (2) Material Properties of the Soil (Nagy. 2015)

Parameter	Value
Young modulus (E)	494 (MPa)
Poisson ratio (ν)	0.17
Density of soil ($\boldsymbol{\rho}$)	1920 (kg/m^3)
Material cohesion (d)	1.38 (MPa)
Material angle of friction (β)	40.4°
Cap eccentricity parameter (R)	0.3
Initial cap yield surface position (ξ_v)	0.02
Transition surface radius parameter (α)	0.01
Cap hardening behavior (stress, plastic volumetric strain)	2.75 (MPa), 0.00 4.83 (MPa), 0.02 5.15 (MPa), 0.04 62.0 (MPa), 0.08

2.2.3- Reinforced Concrete Model:

2.2.3.1- Steel Reinforcement Model:

The Rebar option is used to model the reinforcement of the lining, which is simulated as a layer of a constant thickness equal to the product of the reinforcement area divided by the section's length. The reinforcement ratio arranges between the minimum and maximum ratios adopted by (Code, S. E. B. 2004) as a study parameter. The minimum ratio equals $\mu_{s,min} = 0.0015$, where the maximum equals $\mu_{s,max} = 0.5 * \left(\frac{455}{630+f_y} * \frac{f_c'}{f_y}\right)$ as the lining is considered a slab. The model parameters used for the reinforcement are presented by (Nagy et al. 2010) as γ_{st} = 7800 (kg/m^3), Young modulus (E) = 200000 (MPa), poison's ratio (ν)= 0.3, and yield stress (f_y) = 220 MPa.

The adopted thicknesses of reinforcement layers are shown in Table.3, where a lining without any reinforcement is modeled (case: AS_0) to exhibit the effect of reinforcement.

Table (3)Thicknesses of Steel Layers as Case Studies

Case	Thickness of Steel Layer (mm)
AS_0	-
AS_1	8
AS_2	12
AS_{max}	28

2.2.3.2- Concrete Model:

The concrete lining of the structure is modeled by the Concrete Damaged Plasticity constitutive model. This model provides a general capability for modeling concrete in all types of structures (beams, trusses, shells, and solids), which uses concepts of isotropic damaged elasticity in combination with isotropic tensile and compressive plasticity for the realistic simulation of concrete behavior. It can be used with rebar to model concrete reinforcement with the desired ability to apply in structures subjected to dynamic loading. The parameters adopted for a concrete grade of B50 as presented by (Nagy et al. 2010), and shown in Table.(4).

2.2.4- Soil Structure Interaction:

Simulating the interaction of the structure with the surrounding soil by defining the appropriate properties between the contact surfaces is a vital matter. The more realistic the simulation, the more reliable the results are for the dynamic response of the structure (Nagy et al. 2010). Thus, a formulation that allows for any arbitrary motion of the surfaces such as separation, sliding, rebound, and rotation of the surfaces in contact, should be utilized. In this study, the coulomb friction model is used. The previous theory means a critical shear stress $\boldsymbol{\tau}_{cr}$, at which sliding of the surfaces begins, is a portion of the contact pressure ($\boldsymbol{\tau}_{cr} = \boldsymbol{\mu}$P, where $\boldsymbol{\mu}$ = 0.5 is defined as the coefficient of the friction (Nagy et al. 2010).

Table (4) Material Properties of the Concrete Lining (Nagy et al. 2010)

Parameter		Value	
Young's modulus (E)		19700 (MPa)	
Poisson's ratio (ν)		0.19	
(β)		38°	
Flow potential eccentricity (ε)		1	
F_{b0}/F_{C0}		1.12	
K_C		0.666	
Density		2500 (kg/m^3)	
Concrete compression hardening		Concrete compression damage	
Stress [Pa]	Crushing strain	Damage	Crushing strain
15000000	0.0	0.0	0.0
20197804	0.0000747307	0.0	0.0000747307
30000609	0.0000988479	0.0	0.0000988479
40303781	0.000154123	0.0	0.000154123
50007692	0.000761538	0.0	0.000761538
40236090	0.002557559	0.195402	0.002557559
20236090	0.005675431	0.596382	0.005675431
5257557	0.011733119	0.894865	0.011733119
Concrete tension stiffening		Concrete tension damage	
Stress [Pa]	Crushing strain	Damage	Crushing strain
1998930	0.0	0.0	0.0
2842000	0.00003333	0.0	0.00003333
1869810	0.000160427	0.406411	0.000160427
862723	0.000279763	0.69638	0.000279763
226254	0.000684593	0.920389	0.000684593
56576	0.00108673	0.980093	0.00108673

2−Discussion and Result −2

This issue will be investigated according to the dynamic loads only as the response from static loads with small values compared to the expected from dynamic loads.

3.1- Formation of the Crater:

The crater formation results in a diameter of D_r= 2.24 (m) at a time of t = 12 (ms). Numerical modeling has shown no obvious differences in crater formation after this exact time, which is coincident with the result obtained by (Nagy et al. 2010) in terms of formation time, but with a slight difference not over 2% in diameter. Here we mention that the diameter value falls within the acceptable range due to the different weights of TNT charge obtained by (Nagy. 2015). Fig (3) Shows crater formation.

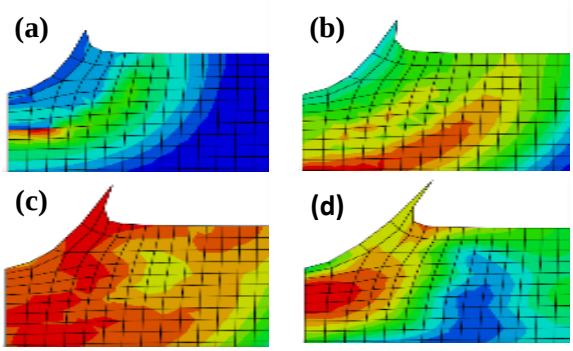

Fig (3) Crater Formation at: (a) t = 4 ms, (b) t = 6 ms, (c) t = 8 ms, (d) t = 12 ms

3.2- Propagation of Blast Waves in the Soil Medium:

To calibrate the direct blast wave in the soil, a set of target points is selected that lie on an inclined line at an angle of 45° to the ground surface as shown in Fig.1(a) (Nagy et al. 2010). These points are located to be remote from free surface and boundary conditions (Nagy et al. 2010, TM 5-855-1 1986), and positioned away from the detonation center with a distance ranging from R= 0.9 m_8m. The empirical governing equation adopted to predict the direct blast wave pressure in a soil medium as given in the design manual (TM 5-855-1 1986) as follows:

$$P\_P = f * A * (\rho\_C\ ) * (R/W\hat{}(1/3)\ )\hat{}(-n)$$

Where; f = a coupling factor, A = a constant, $\boldsymbol{\rho}$c= the acoustic impedance, R = the distance from the charge center, W = the explosive mass, and n = a constant attenuation factor. Or might be written as follows (Nagy et al. 2010):

$$P\_P = C * (R/W\hat{}(1/3)\ )\hat{}(-n)$$

Where; (C) is a constant that depends on the properties of soil and charge material (TM 5-855-1 1986), and the attenuation factor (n) depends on the soil properties (Bulson. 1991, TM 5-855-1 1986). In this paper, the constants adopted for this investigation as presented by (Nagy et al. 2010) and shown in Table.5, even though there are a lot of studies to re-examine the peak pressure in soils due to the previous equation (Leong et al. 2007, Yankelevsky et al. 2011). The following Fig.4 shows the results of numerical peak pressures due to the free field calibration, which can be

expressed by using the best fit line. The values of the numerical constants fall in the acceptable range between the limits of the experimental ones.

Table (5) Constants of Peak Pressure Equation

State	c	n
The empirical upper limit (Nagy et al. 2010)	1.12	2.75
The empirical lower limit (Nagy et al. 2010)	0.65	2.5
The numerical result	0.8896	2.538

The previous results are also achieved in the scatter field (existence of structure).

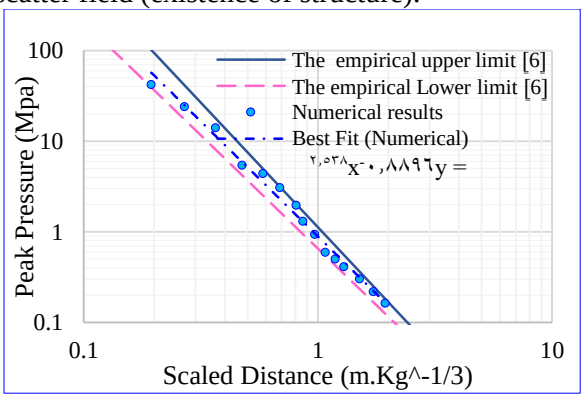

Fig(4) Free Field Calibration

Fig.5(a) shows the vertical displacement of the soil and the lining at the exact contact point of the center of the lining roof with the surrounding soil. The lining separates of the soil and then rebounds again, where the sliding can be clearly shown in Fig.5(b).

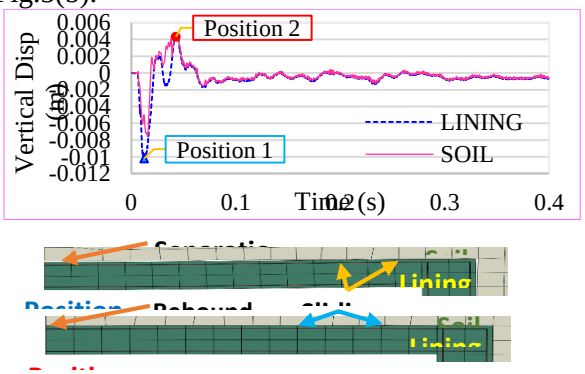

Fig(5)Interaction of the Lining with the Soil for Structure Depth d_1 = 4m, and Case AS_1; (a): Vertical Displacements at the Contact Point of the Lining Center with the Soil, (b): Interaction Properties

(b)

Due to previous results, it is clear that this complete coupled numerical model can represent the dynamic behavior of the problem.

3.3- Structure Response:

A set of target points on the roof slab is selected to study the dynamic response of the structure as the roof is the most critical element due to the explosive charge positioned above its center (Nagy et al. 2010). These points are: (1) the center point, (2) the quarter span roof point, and (3) the corner roof point as shown in Fig.1(a). The effect of the reinforcement ratio of the lining is conducted considering the first depth of the structure (d_1 = 4 m), then the effect of the depth on the dynamic response is proposed by increasing the depth from d_1 = 4 m to d_2 = 8 m.

3.3.1- The Effect of Reinforcement Ratio:

The reinforcement ratios lie in between the minimum and maximum ones (Code, S. E. B. 2004). Fig.6 (a, b, and c) shows the vertical displacements at the target points for all cases of reinforcement, taking into account the first depth of structure d_1 = 4 m, and indicates that as the ratio increases, the peak of displacements is less remarkably with final permanent ones, the same result has obtained for lateral displacements. The residual displacement for the case AS_0 is the largest in order of about 9 mm for point (1) and about 3 mm for point (2) while for point (3) is about 1.5 mm, which gives a perception of large damage or failure in the lining roof for this case. Fig.7 shows the damage to the concrete lining. It can be noted that the greatest expected damage occurs at point (1), where the damage has been evaluated concerning previous reinforcement ratios and shown in Fig.6 (d). It is clear that as the ratio of reinforcement increases the damage index decreases.

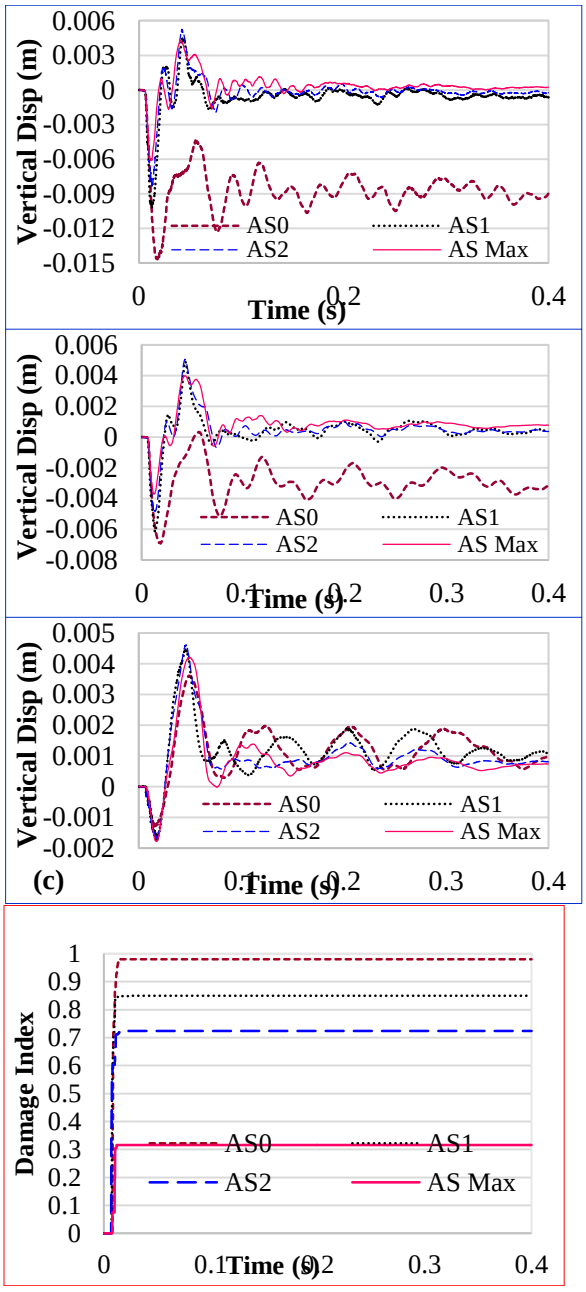

Fig (6) Vertical Displacements; (a): Point 1, (b): Point 2, (c): Point 3; and Damage Evaluation; (d): Damage Index at Point 1; Structure Depth d_1 = 4 m

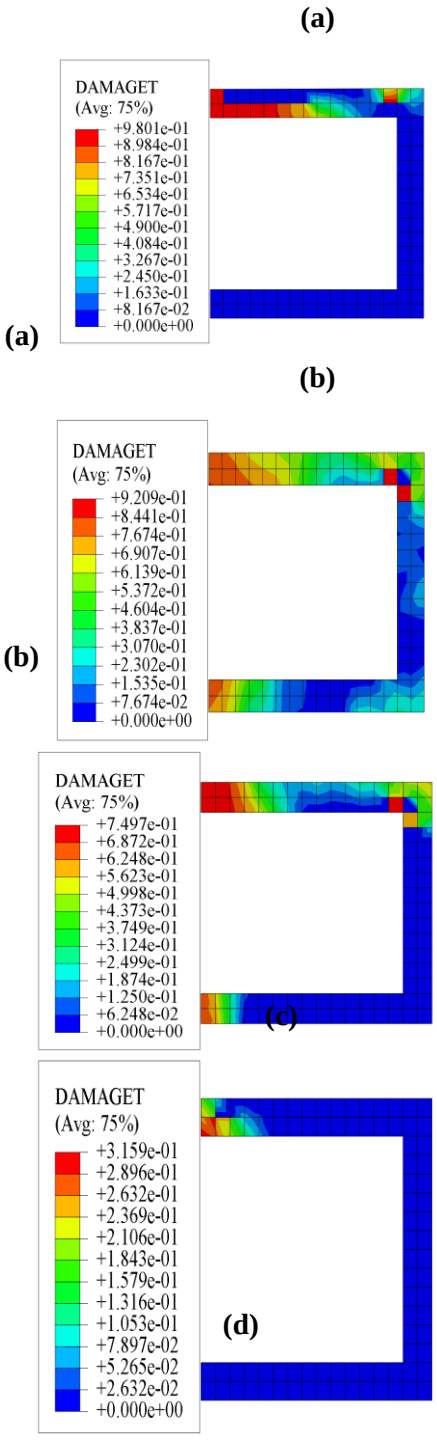

Fig (7) Damage in the Concrete Lining; Structure Depth d_1 = 4 m, and Reinforcement Cases; **(a): AS_0, (b): AS_1, (c): AS_2, (d): AS_{max}**

A damage index value equal to (1) means a complete loss of strength, the value of (0) reflects no damage occurs while the value of (0.7) informs

severe damage and the beginning of failure (Kim et al. 2005), therefore the roof has already been damaged and begun to collapse, especially if the static loads are taken into account, for cases (AS_0, AS_1, and AS_2) in this investigation, while using the maximum ratio (case AS $_{max}$) has confined the damage to the most critical area of the roof which is around the point (1) with a damage index value not exceeding (0.32) and the lining becomes within the limits of relative damage away from the beginning of failure. It is useful to note that Fig.7 indicates the emergence of critical areas outside the roof center, such as the floor center and the joint (roof_ wall) for cases (AS_1 and AS_2).

3.3.2- The Effect of Structure Depth:

Fig.8 shows the vertical displacements of the most critical area of the roof at point (1) for each reinforcement ratio and depth. As the depth increases to $d_2 = 2\ d_1$, the vertical displacements decrease significantly, with a peak reduction percentage of about 70% for all reinforcement cases, but still having a final residual displacement, the same as for lateral ones. The damage evaluation has been also conducted for the structure at depth $d_2 = 8$ m as shown in Fig.9, while Fig.10 exhibits the damage index of the roof at point (1) concerning different reinforcement ratios and depths.

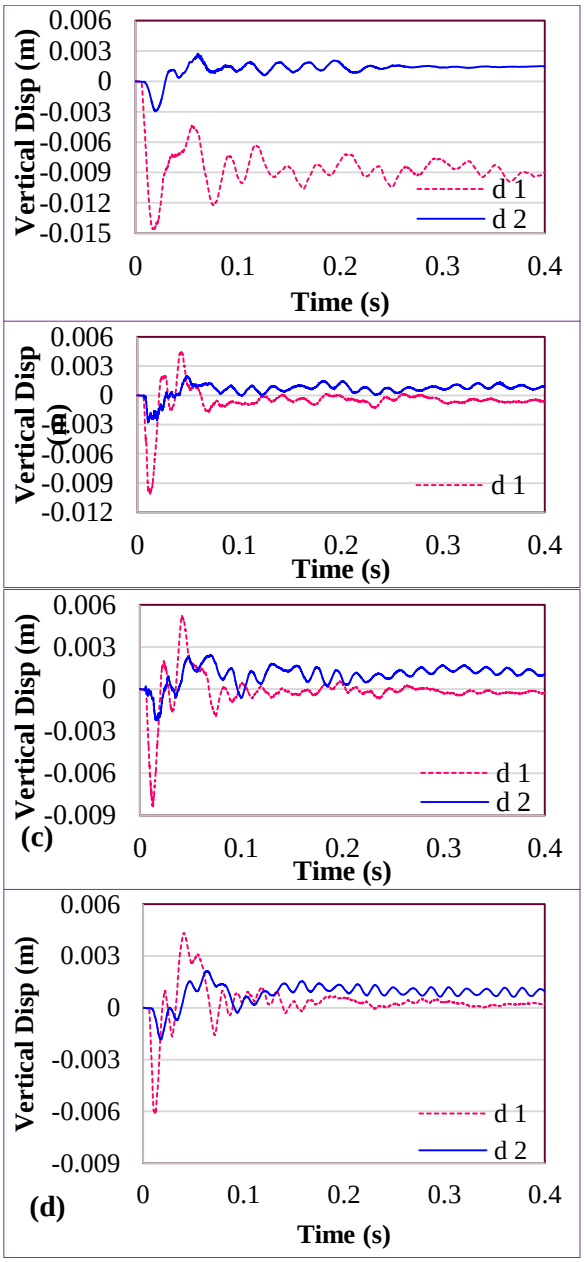

Fig (8) Vertical Displacements at Point (1); Depth of Structure ($d_1 = 4$ m **&** $d_2 = 8$ m**),** and Reinforcement Cases; **(a): AS_0, (b): AS_1, (c): AS_2, (d): AS $_{max}$**

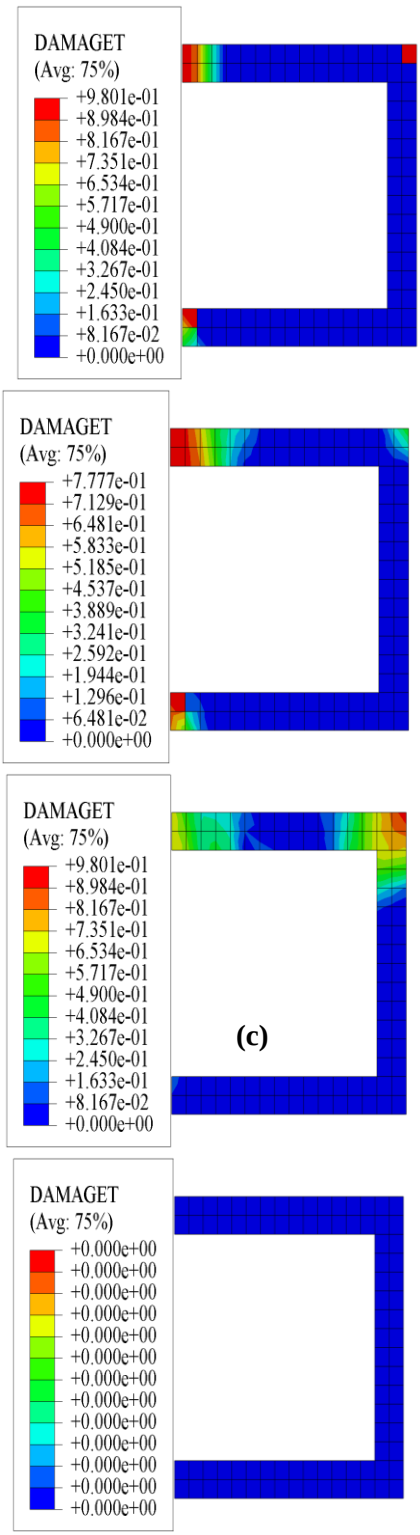

Fig(9)Damage in the Concrete Lining; Structure Depth d_2 = 8 m, and Reinforcement Cases; **(a): AS_0, (b): AS_1, (c): AS_2, (d): AS_{max}**

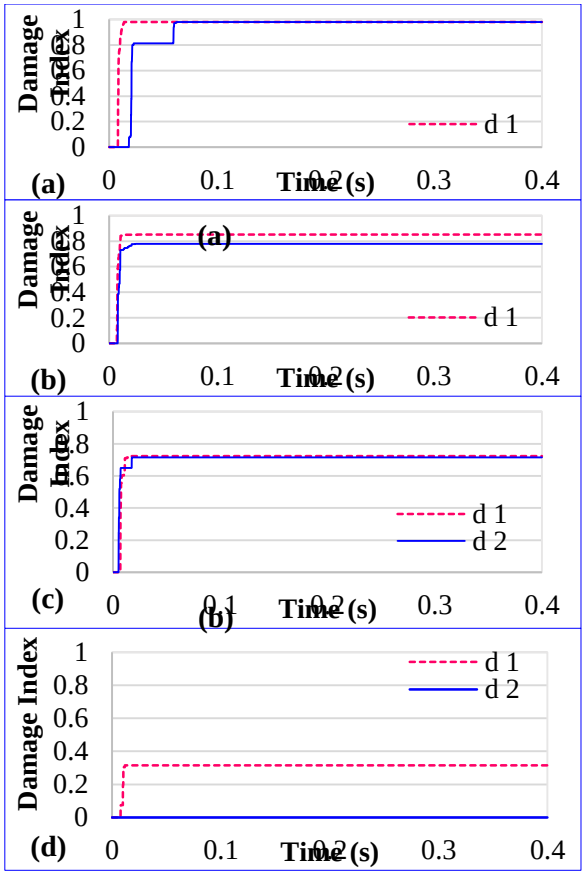

Fig (10) Damage Index of the Concrete Lining at Point (1); Structure Depth (d_1= 4 m & d_2= 8 m), and Reinforcement Cases; **(a): AS_0, (b): AS_1, (c): AS_2, (d): AS_{max}**

Due to the damage evaluation, by increasing depth, it is clear that the lining still has been damaged and has begun to collapse at the roof center for cases (AS_0, AS_1, and AS_2), but with a slight difference manifested as a reduced main damaged roof area. The damage is more confined to the roof center /point(1)/, with an additional collapsed area at the roof corner /point (3)/ for cases (AS_0 and AS_2). The results also inform that the lining for the case (AS_{max}) is completely safe with no damage occurrence by increasing depth.

Funding: This Research Is Funded By Damascus University Funder No (50110002059.

3- Conclusion:

Due to the investigation of the proposed case study in this paper:

- As the reinforcement ratio increases, the peak of displacements decreases significantly but with residual displacements which indicate a damage occurrence. By evaluating the damage, it has been found that as the reinforcement ratio increases to the maximum, the damage index value decreases so that the lining becomes within the limits of relative damage away from collapse.
- As the depth of the structure increases from (d_1) to ($d_2 = 2*d_1$), the peak of displacements decreases by about 70% for all reinforcement ratios but with still residual displacements and a decline in the most critical damaged area, except for the maximum reinforcement as the lining becomes within the safe limits without any damage.
- It is beneficial to note the emergence of severely damaged areas outside the expected so-called most critical areas.
- Based on the former, when designing the buried facilities, it is necessary to achieve an optimum design point, in terms of structure depth and utilized reinforcement ratio, which leads to safe facilities or acceptable relative damage.

References:

Bulson, P. S. (1997). Explosive loading of engineering structures. CRC Press.

Code, S. E. B. (2004). Syrian engineering association publications. Damascus, Syria (In Arabic).

Hu, Y., & Randolph, M. F. (1998). A practical numerical approach for large deformation problems in soil. International Journal for Numerical and Analytical Methods in Geomechanics, 22(5), 327-350.

Kim, T. H., Lee, K. M., Chung, Y. S., & Shin, H. M. (2005). Seismic damage assessment of reinforced concrete bridge columns. Engineering Structures, 27(4), 576-592.

Leong, E. C., Anand, S., Cheong, H. K., & Lim, C. H. (2007). Re-examination of peak stress and scaled distance due to ground shock. International journal of impact engineering, 34(9), 1487-1499.

Nagy, N., Mohamed, M., & Boot, J. C. (2010). Nonlinear numerical modelling for the effects of surface explosions on buried reinforced concrete structures. Geomechanics and Engineering, 2(1), 1-18.

Nagy, N. M. (2015). Numerical Evaluation of Craters Produced by Explosions on the Soil Surface. Acta Physica Polonica, A., 128.

Station, U. A. E. W. E. (1986). Fundamentals of protective design for conventional weapons (TM 5-855-1). Vicksburg: US Department of Army.

Systèmes, D. (2014). ABAQUS/Standard User's Manual, Version 6.14. Simulia, Providence.

Wolf, J. P. (1985). Dynamic soil-structure-interaction Englewood Cliffs. Inc., Prentice-Hall, New Jersey.

Yang, Y., Xie, X., & Wang, R. (2010). Numerical simulation of dynamic response of operating metro tunnel induced by ground explosion. Journal of rock mechanics and geotechnical engineering, 2(4), 373-384.

Yankelevsky, D. Z., Karinski, Y. S., & Feldgun, V. R. (2011). Re-examination of the shock wave's peak pressure attenuation in soils. International journal of impact engineering, 38(11), 864-881.